A Label-free Nanostructured Plasmonic Biosensor based on Blu-ray Discs with integrated microfluidics for sensitive biodetection

Gerardo A. López-Muñoz,[a,b] M. Carmen Estevez,[b,a] E. Cristina Peláez-Gutierrez,[a,b] Antoni Homs-Corbera,[a] M. Carmen García-Hernandez[c] and J. Ignacio Imbaud[c] and Laura M. Lechuga[a,b]

[a]Nanobiosensors and Bioanalytical Applications Group (NanoB2A), *Catalan Institute of Nanoscience and Nanotechnology (ICN2), CSIC and the Barcelona Institute of Science and Technology*, 08193 Bellaterra (Barcelona), Spain

[b]CIBER-BBN Networking Center on Bioengineering, Biomaterials and Nanomedicine, Spain

[c]Protein Alternatives, S.L., Tres Cantos, Madrid, Spain

Abstract. In order to achieve fully operative lab-on-a-chip (LOC) biosensor platforms several challenges need to be surpassed, as having high-throughput and low-cost sensor fabrication techniques and microfluidics and optical subsystems integration. Nanostructure-based plasmonic biosensors have quickly positioned themselves as interesting candidates for the design of portable optical biosensor platforms considering the potential benefits they can offer in miniaturization, multiplexing, real-time and label-free detection. We have developed a simple integrated nanoplasmonic sensor taking advantage of the periodic nanostructured array of commercial Blu-ray discs. Sensors with two gold film thicknesses (50 and 100 nm) were fabricated and optically characterized by varying the oblique-angle of the incident light in optical reflectance measurements. We observed an enhancement in sensitivity and a narrowing of the resonant linewidths as the light incidence angle was increased, which could be related to the generation of Fano resonant modes. The new sensors achieve a figure of merit (FOM) up to 35 RIU^{-1} and a competitive bulk limit of detection (LOD) of 6.34×10^{-6} RIU. The integrated chip is only 1 cm^2 (including a PDMS flow cell with a 50 μm height microfluidic channel fabricated with double-sided adhesive tape) and all the optical components are mounted on a 10 cm×10 cm portable prototype, illustrating its facile miniaturization, integration and potential portability. Finally, to assess the label-free biosensing capability of the new sensor, we have evaluated the presence of specific antibodies against the GTF2b protein, a tumor-associate antigen (TAA) related to colorectal cancer. We have achieved a LOD in the pM order and have evaluated the feasibility of directly evaluating biological samples such as human serum.

Keywords:

Blu-ray disc; plasmonic nanostructure; integration, microfluidics; biosensing; antibody

Introduction

Nowadays there is increasing interest to develop biosensor devices providing medically relevant sensitivity and real-time response in a cost-effective manner for portable point of care (POC) platforms[1]. Optical biosensors based on Surface Plasmon Resonance (SPR) and particularly those using metallic nanostructures, have undergone an extensive development because they are promising biosensing platforms due to their low-complexity detection schemes and a well-established surface functionalization protocols[2,3]. However, in order to achieve fully operative lab-on-a-chip (LOC) biosensor platforms several challenges need to be surpassed, as using high-throughput and low-cost sensor fabrication techniques and an effective microfluidics and optical subsystems integration [1]. There have been some interesting approaches that try to solve these aspects, (specially the optics and the microfluidics integrated on chip) and, although they demonstrated biosensing capabilities, they eventually use bulky detection schemes[4,5]. More integrated designs with reduced dimensions and simple instrumentation have been reported based on imaging systems. However most of them have limited sensitivity (in the range of 10^{-5} RIU) [6,7]. Besides this, improving nanostructures design and performance to push sensitivity levels is currently under exhaustive research. During last years the development of novel fabrication methods and nanostructures with promising performance have been reported[8-12]. Nevertheless most of them still involve complex and expensive fabrication processes[13-15], which limit their applicability outside the laboratory environment. A simple and cost-effective alternative fabrication method employs industrially produced patterned optical discs, as a nanoslit-containing substrate, to generate the SPR[16,17] phenomena. This approach provides a high degree of controlled reproducibility while affording low-cost fabrication. In general, the bulk sensitivities obtained using optical discs as substrates[16] are similar to those obtained with engineered nanoslits[12,18] making them interesting for many applications, including biosensor devices development. The high availability of optical discs and their convenient standardized mass-production manufacturing processes, make them especially attractive to build sensing platforms for POC devices.

Blu-ray discs in particular are top-down fabricated optical discs consisting of a polycarbonate substrate patterned with highly ordered concentric periodic nanoslits (320 nm period, 160 nm width and ≈20 nm depth)[16,17]. Obtaining plasmonic chips from blue-ray discs involves a simple fabrication process; and recently the possibility to generate plasmonic effects in the visible range when incorporating metal layer films with thicknesses in the range of 50-100 nm[16] has been demonstrated. Blu-ray based chips exhibit a plasmonic band in the visible region. Other commercially available optical discs present plasmonic bands in the near infrared spectra due to larger periods of the structures[16]. Near IR spectrometers commonly are more expensive, which can eventually increase the overall cost of a final device and traditionally they possess lower resolution of the plasmonic detection compared with more convenient conventional visible compact spectrometers. Moreover, the periodic nanostructures present in Blu-ray discs can promote the presence of Fano resonances[19]. This is due to the coupling of the localized resonances in the nanoslits and the Wood´s anomalies present in high ordered nanostructures that behave as a grating[20]. This effect narrows the resonant linewidths and enhances the intensity of the optical fields.

Based on these considerations we present a simple, cost-effective nanostructured plasmonic biosensor based on Blu-ray discs with integrated microfluidics for high performance biosensing. The sensors were fabricated following extremely simple and reproducible processes. We considered different metal layer thicknesses, to evaluate its influence in the optical performance of the nanostructures. The chips were optically characterized under TM polarized white light at different angles of incidence to generate Fano resonant modes and to evaluate their performance as biosensor platforms. We used a wavelength shift interrogation method to optimize the biosensor performance by tuning the optical conditions and the thickness of the nanostructured substrate. We perform three-dimensional finite difference time-domain (FDTD) simulations to evaluate the reflectance spectra and the electric field distributions. With view of achieving a compact operative device, further integration was done by incorporating a 1 cm^2 PDMS flow cell with a patterned microfluidics (single channel

of 50 µm height) obtained using a simple and inexpensive double-sided adhesive tape. All the optical components are fixed on a 10×10 cm^2 portable prototype, illustrating its facile miniaturization, integration and potential portability. The viability of this configuration for biosensing was further explored by performing label-free measurements based on the detection of specific antibodies for GTF2b protein, a tumor-associate antigen (TAA) related to colorectal cancer, achieving LOD in the pM order. We also assessed the feasibility of measuring biological samples by evaluating diluted serum, achieving promising performance in this complex matrix.

Materials and Methods

Fabrication and Integration of Nanostructured plasmonic chip. Single layer recordable Blu-ray discs (TDK, T78088, Japan) were used after removal of their protective and reflective films. These were removed by trimming the disc around the edges and then by immersing it in a hydrochloric acid solution (1 M HCl) for 120 min. After consecutive rinsing with MilliQ water and ethanol and air drying the substrate, gold layers up to 100 nm thickness were deposited by electron beam deposition (1 Å/s). Individual plasmonic chips (size of 1 cm^2) were obtained by cutting the gold-coated optical disc with a conventional computer numerical control (CNC) router (LPKF Laser & Electronics, Protomat C100/HF, Germany). The flow cell for carrying out real time measurements in solution was fabricated by patterning a microfluidic channel (10 mm length, 1 mm width, 50 µm height and 1 µL volume) in a 50 µm thick double-sided adhesive tape sheet (Nitto, D5331,Japan). A polydimethylsiloxane (PDMS) thin layer (2 mm thickness, Dow Corning Co., Sylgard 184, USA) was added as a cover to facilitate the connection of the fluidic tubes. The microchannel was designed to promote laminar flow and to increase the mass transfer near the sensor surface (See Figure 1a).

Experimental setup and optical characterization. The integrated sensor chips were clamped to a custom-made optical platform (Figure 1b). The chips were connected to a microfluidic system consisting of a syringe pump (New Era, NE-1000, USA), with adjustable pumping speed guaranteeing a constant liquid flow, and a manually operated injection valve (Valco Instruments Co. Inc., Cheminert C22-3186, USA). Reflectance measurements were performed under TM-polarization of a compact broadband light source (HL-2000-HP Ocean Optics, US) at different incident angles (ranging from 30º to 70º). The incident excitation plane was perpendicularly aligned to the nanoslits direction. The reflected light was collected and fiber-coupled to a compact CCD spectrometer (Flame-T spectrometer, Ocean Optics, US). All optical components were mounted on a 10 × 10 cm^2 optical platform. Reflectivity spectra were acquired every 3 ms, and 250 consecutive spectra were averaged to generate the spectrum to be analyzed. By using a virtual instrumentation software (National Instruments, Labview, USA) it was possible to track the real-time changes in the resonance peak position (λ_{SPP}) *via* polynomial fit. The bulk refractive index (RI) sensitivity and full width at half maximum (FWHM) of the sensor as a function of the incidence angle, were determined using solutions of glycerol in water (ranging from 4.2 mM to 136 mM, equivalent to a range of RIU between 1.3334 and 1.3463 RIU).

FDTD Simulations. Three-dimensional FDTD simulations were performed using commercial software (Lumerical Inc., FTDT solution, Canada). Structural parameters of the Blu-ray discs were used in the simulations (i.e. a slit period of 320 nm, slit width of 160 nm and a height of 20 nm). Periodic boundary conditions were used in x and y axis, and perfect matched layers (PML) approach was used in the z axis, with a uniform mesh size of 2 nm in all axis. The optical constants of the polycarbonate and gold were considered from Sultanova[21] and Johnson and Christy[22], respectively, in the range from 400 nm to 1000 nm, under TM-polarized light with an oblique light incidence angle of 70º.

Surface functionalization and GTF2b detection assays. Alkanethiol for self-assembled monolayer (SAM) formation (16-mercaptohexadecanoic acid, MHDA), (1-ethyl-4 (3-

dimethylaminopropyl) carbodiimide hydrochloride (EDC) and N-hydroxysulfosuccinimide (s-NHS) for carboxylic groups activation, ethanolamine and Tween 20 were acquired to Sigma–Aldrich (Germany). Poly(L-lysine)-graft-poly(ethylene glycol) co-polymer (PLL-PEG, MW∼70000 g mol^{-1}) was purchased to SuSoS AG (Switzerland). Commercial serum was obtained from Sigma–Aldrich (Germany). Antibody anti-GTF2b was purchased to Santa Cruz Biotechnology (USA). GTF2b protein was produced in bacterial expression systems. The coding sequence of the DNA was cloned into pET28a(+) expression vector (Novagen) and transformed into protease deficient BL21(DE3) competent *E. coli* cells (Invitrogen). The protein was overexpressed in cultures of Luria Broth media (Pronadisa) containing kanamycin (Sigma-Aldrich) by inducing the strain with 0.8 nM of IPTG (Apollo Scientific Ltd). Bacterial pellets were then disrupted by sonication in buffer containing 20 mM sodium phosphate pH 7.4 (Merck), 500 mM NaCl, 0.5 mM EDTA, 1 mM DTT, 0.010 g PMSF (Sigma-Aldrich), 1X Complete^{TM} protease inhibitors (Roche), 0.25 mg/mL lysozyme (Sigma-Aldrich), 1% N-Lauroylsarcosine (Sigma-Aldrich) and 1% Triton X-100 (Sigma-Aldrich). The lysate was clarified by centrifugation and filtered through a 0.45 µm pore-size syringe filter (Sarstedt). The protein contained in the soluble fraction was purified by affinity chromatography (IMAC) using an ÄKTA FPLC system and HisTrap FF Crude columns (GE Healthcare). Purified GTF2b protein was eluted in PBS 1X, 0.1 M Arginine (Alfa Aesar), 150 mM Imidazole (Sigma-Aldrich), 1 mM DTT, 0.5 mM EDTA and 1X Complete^{TM} protease inhibitor, pH 7.4. The protein was dialyzed in PBS 1X before use in the biosensing experiments.

Sensor chips (100 nm thickness gold layer) were cleaned and activated for surface functionalization by performing consecutive 1 min sonication cycles in ethanol and MilliQ water, drying with N_2 stream and finally by placing them in a UV/O_3 generator (BioForce Nanoscience, USA) for 30 min. An alkanethiol SAM with reactive carboxylic groups was obtained by coating the sensor chip with 500 µM MHDA in ethanol overnight at room temperature. Then, the surface was rinsed with ethanol and dried with a N_2 stream. Prior to

the biofunctionalization step, the chip was bonded to the microfluidics and placed in the optical platform. The immobilization of the GTF2b protein was performed *in situ*, and was continuously monitoring in real time. For the activation of the carboxylic groups a solution of 0.2 M EDC/0.05 M s-NHS in MES buffer (100 mM pH 5.5) was injected and flowed over the SAM monolayer at 20 µL/min (using H_2O as running buffer). Subsequently, a 50 µg/mL GTF2b protein solution in PBS (10 mM pH 7.4) was injected and flowed at 5 µL/min. Finally, a blocking solution (ethanolamine, 1M pH 8.5) was injected for 2 min at 25 µL/min. After immobilization, PBST 0.5% (PBS 10mM pH 7.5 +0.5% Tween 20) was settled as running buffer. For optimization and assessment studies, different concentrations of specific antibody diluted in PBST 0.5% were flowed over the functionalized surface at 25 µL/min. Regeneration of the surface was achieved by injecting 20 mM NaOH at 65 µL/min. Calibration curves were fitted to a one-site specific binding model. LOD and LOQ (Limit of quantification) were calculated as the concentration corresponding to the blank signal plus three and ten times its standard deviation (SD), respectively. For the evaluation in serum, an additional blocking step was considered according to previous results[23] based on the addition of a PLL-PEG solution (0.25 mg/mL) to minimize non-specific adsorptions.

Results and Discussion

Characterization and simulation of nanostructured plasmonic sensor.

Gold capped nanoslits were fabricated taking advantage of the precise and large area of nanostructured array present in commercial Blu-ray discs. Two gold film thicknesses (50 and 100 nm) were selected for the fabrication of the chips. These dimensions were selected according to previous results[16] that showed no significant differences in RI sensitivity for Blu-ray discs with metal layers thicknesses between 60 and 120 nm in reflection measurements at normal light incidence. Different angles of incident light (between 30º-70º) were studied for the reflection measurements in order to evaluate its influence in the sensing performance

due to the generation of other resonant modes under oblique-angle incident light. Optical characterization of the integrated sensors was performed under TM-polarized broadband light. Reflection spectra were collected in air (η=1.00) and water (η=1.33).

Figures 2a and 2b show the reflectance spectra for both thicknesses. First, a shift of the resonance peak λ_{SPP} to higher wavelengths is observed as the incidence angle increases. Also in both cases narrower resonant linewidths are observed, with a decrease in the full width at half maximum (FWHM). This behavior can be correlated with the possibility to induce Fano resonances in periodic nanoslits[18,24]. These resonant modes narrow the resonant linewidths and enhance the intensity of the optical fields. This enhancement is due to the coupling of the localized resonances in the nanoslits and the Wood´s anomalies promoted by the high ordered periodic nanostructures of the Blu-ray discs that behave as a grating[24]. The generation of the plasmonic effect for high order periodic nanostructures can be described by the Bloch wave surface plasmon polaritron (BW-SPP), when the Bragg condition for one-dimensional periodic metallic structure is satisfied[18,24]. Under oblique-angle incident light, it can be described by the following equation:[24]

$$\lambda_{SPP} = \frac{P}{i}\left\{Re\left[\left(\frac{\varepsilon_m n^2}{\varepsilon_m + n^2}\right)^{1/2}\right] \pm \sin\theta\right\} \quad (1)$$

Where *i* is the resonant order, *P* is the period of the nanostructure, ε_m is the dielectric constant of the metal, *n* is the environmental refractive index and θ is the incident angle, respectively.

A red-shift in the resonant wavelength is expected when the RI of the medium near the gold surface increases. Also, for a given nanostructure period, the resonance wavelength is controlled by the light incident angle. The narrowing in the resonance peak with the increase in the incident angle is related to the interaction of the different resonance modes: Wood´s anomalies in periodic nanostructures, and the BW-SPP on the periodic surface. By increasing the incident angle, the BW-SPP at the metal/substrate interface interacts with the

substrate modes[24]. This interaction between different modes produces Fano resonances with narrower resonant linewidths[24,25]. Moreover, by increasing the angle of the incident light, the optical energy scattered from one nanostructure can be collected by neighboring nanostructures, decreasing radiative loss[26].

The influence of the angle of the incident light and the thickness of the metal layer was also studied by evaluating aqueous solutions with different RI. From the generated spectra, both bulk RI sensitivity and FWHM were extracted and the FOM estimated. As can be observed in Figure 2c, a higher incident angle promotes an increase in sensitivity and a decrease in FWHM for both thicknesses. Maximum bulk sensitivity and minimum FWHM values were obtained at 70° incident angle of light. A high incident angle increases the possibility to reach higher FOM with these sensors and an enhancement in optical fields due to longer plasmon lifetimes[26]. Sensitivity values of ≈ 425 nm·RIU^{-1} and 360 nm·RIU^{-1} with FWHM values of 12 nm·RIU^{-1} and 15 nm·RIU^{-1} were achieved for 100 nm and 50 nm gold layer thickness, respectively. These behaviors are correlated with the fact that a thin gold layer promotes interaction of plasmons with the underlying substrate with more radiative losses. This could explain a higher FWHM in 50 nm gold layer thickness sensor and lower bulk sensitivity due to a decrease in the intensity of the optical fields[24]. This behavior is also correlated with the improvement in the sensing performance observed at higher incidence angle. Under these conditions, the interaction between nanostructures increases and the optical energy scattered or their loss as free-space light is reduced, therefore promoting the enhancement of the optical fields[26].

The experimental results were contrasted with reflectance spectra and optical field distributions calculated from FDTD simulations. As can be observed in Figure 3a there is a good agreement between the calculated and the experimental reflectance spectra, with a narrower resonant linewidth for 100 nm gold thickness film compared to the 50 nm gold film. As previously discussed, this behavior could be related to the interaction of plasmons with the underlying substrate. To evaluate this possibility we analyzed the electric field

distributions calculated from FDTD simulations. Figures 3b and 3c illustrate the differences in the electric field distributions for a gold thickness layer of 50 and 100 nm, respectively. The interaction of plasmons with the underlying substrate is obvious for the 50 nm gold layer, which prones radiative losses and decreases the intensity of the optical fields with shorter decay lengths. On the other hand, for a 100 nm gold layer a greater intensity and longer decay lengths are observed. The observed changes in the electric field distribution and in the interaction with the underlying substrate with the metallic thickness layer imply the possibility to tune the evanescent field decay length of the nanostructure. By controlling the evanescent field decay length modifying the metal thickness layer, it could be possible to detect targets with different sizes, as has been previously proposed[27,28].

Considering the performance of the sensors, a FOM up to 35 RIU^{-1} is achieved for the 100 nm thickness with a bulk sensitivity of 425 $nm \cdot RIU^{-1}$ (Figure 4) and a LOD up to $6.34 \cdot 10^{-6}$ RIU for the configuration with a 70 degrees light incidence angle. This value is highly competitive and comparable to the current state of the art in SPR [1,3] and to some engineered nanoslit based sensors[12.18] but offering at the same time a simpler and more compact prototype. This excellent performance can also be correlated with the good S/N ratio obtained, as can be observed in the real-time sensograms (see Figure 4a) with a noise standard deviation in the range of 4.32×10^{-4} nm. The enhancement inbulk sensitivity and FOM with the increase in the incidence angle confirms that oblique incidence can increase the sensing performance parameters of these metallic nanostructures taking advantage of the generation of Fano resonant modes. The batch to batch fabrication reproducibility is one of the main challenges to demonstrate how to achieve high-throughput nanostructured-based plasmonic biosensors, crucial for a future POC device. The reproducibility of the fabrication process was assessed by recording and analyzing the reflectance spectra of nine samples from three different fabrication batches using the same experimental setup. Analyzing the reflectance spectra presented in Figure 5a, a mean λ_{SPP}, of 635.32 ± 0.61 nm and FWHM value of 10.12 ± 0.94 were obtained. Figure 5b shows a very low dispersion in

both parameters for the nine samples. Overall, taking advantage of the high-throughput fabrication process of Blu-ray discs at industrial scale, which is completely stablished, together with the simple steps necessary to obtain the final nanoslits (only cleaning and evaporation steps) contribute to the achievement of highly reproducible substrates from batch to batch. Given this simple and cost-effective fabrication process, together with a straightforward integration using inexpensive microfluidics and a detection scheme with extra miniaturization potential, our sensor is a promising candidate for POC platforms.

Biosensing evaluation with the integrated platform

The potential of the developed integrated plasmonic device for biosensing applications was assessed by employing an assay for the early detection of colorectal cancer based on the detection of specific autoantibodies against tumor associated antigens (TAA). TAAs are overexpressed proteins associated with malignant growth. GTF2b protein (general transcription factor IIB) is a suspected TAA related to colorectal cancer. The detection of the TAAs is highly interesting for early cancer detection. However, these TAAs become even more relevant since some cancers have demonstrated to be immunogenic, so that they can stimulate the immunoresponse, triggering the generation of specific autoantibodies by the human immunosystem. Therefore, the detection in a patient's blood sample of the generated autoantibodies against these TAAs is even more remarkable as they can be detected at higher concentrations and at very early stages of the disease compared to TAAs. Additionally, autoantibodies possess a higher molecular weight, being more suitable for mass-dependent label-free refractometric configurations. A nanostructured substrate with higher bulk sensitivity (gold film of 100 nm) was modified by forming a SAM with carboxylic acid, which was further activated and reacted with the GTF2b protein. The immobilization was monitored in real time, as can be seen in Figure 6a. The detection of the specific antibody associated to this protein shows a good dose-response relation for different

concentrations of antibody (see figure 6b). Given the excellent signal to noise (S/N) ratio obtained with the setup and the processing software (~1.09 pm) we were able to achieve a LOD of 3.42 ng/mL (22.6 pM) and a LOQ of 11.45 ng/mL (75.6 pM), respectively (see in Figure 6c the calibration curve). The values are slightly better than the ones that we previously obtained for the same assay but with gold nanodisks as substrate using an optical setup under prism-coupled TIR (total internal reflection) measurements[23]. Whereas gold nanodisks offer excellent properties, this new approach provides an even faster and highly reproducible fabrication method and minimizes the optical setup complexity being unnecessary the use of coupling components. In order to preliminary assess also the feasibility of measuring biological samples, an additional blocking step was considered based on the addition of a layer of PLL-PEG, a well-known compound able to minimize nonspecific adsorptions in complex media[18]. Although the blocking did not completely remove the binding of serum components, resulting in a shift around 0.17 nm for 10% serum (see Figure 6d, black line) it did not affect the target detection in buffer. As can be seen in Figure 6d (green and orange lines) similar shift was observed before and after blocking, being around 0.5 nm in both cases. When measuring in diluted serum (blue line in figure 6d) a total signal of ~ 0.68 nm was observed, which corresponds to the contribution of both the serum ($\Delta\lambda$~ 0.17 nm) and the specific target binding ($\Delta\lambda$ ~ 0.5 nm). Overall these results reflect the promising performance of this kind of easy-to-fabricate nanostructures, with high potential to implement low cost competitive devices for relevant clinical applications.

Conclusions

A simple label-free integrated plasmonic biosensor based on commercial Blu-ray discs has been demonstrated. An enhanced sensitivity was achieved by exploiting the Fano resonant modes generated in the metallic nanostructures under oblique-angle of the incident light. In contrast to other engineered nanoslits based sensors, we took advantage of the high-throughput fabrication process of Blu-ray discs at industrial scale, to achieve highly reproducible substrates from batch to batch. A FOM up to 35 nm^{-1} and a bulk limit of

detection (LOD) up to 6.34×10^{-6} RIU were obtained. The achieved LOD is in general within the same order of magnitude or even one order of magnitude better than some reported instruments. To evaluate the label-free biosensing capability of the integrated chip (only 1 cm^2, including a microfluidics pattern) we also proved the real-time detection of specific antibodies for a tumor-associate antigen (GTF2b antigen). A LOD in the pM order was obtained and we observed a promising performance in diluted serum, which reinforces the future applicability of this prototype. Given the simplicity, reproducibility and the low cost of the sensor fabrication process, together with its straightforward integration, the presented device is a promising candidate for the development of competitive POC platforms.

Acknowledgements

GL acknowledges financial support from CONACYT 225362 scholarship. We acknowledge the financial support from COLONTEST project (RETOS-COLABORACIÓN Subprogram, RTC-2014-1518-1). The NanoB2A is a consolidated research group (Grup de Recerca) of the Generalitat de Catalunya and has support from the Departament d'Universitats, Recerca i Societat de la Informació de la Generalitat de Catalunya (2014 SGR 624). ICN2 is the recipient of Grant SEV-2013-0295 from the "Severo Ochoa Centers of Excellence" Program of Spanish MINECO.

References

1. Lopez, G., Estevez, M.-C., Soler, M., Lechuga, L. M. (2017) Recent advances in nanoplasmonic biosensors: applications and lab-on-a-chip integration. *Nanophotonics*, 6(1), 123-136.
2. Tokel, O., Inci, F., Demirci, U. (2014) Advances in plasmonic technologies for point of care applications. *Chem. Rev.*, 114(11), 5728-5752.
3. Estevez, M.-C., Otte, M. A., Sepulveda, B., Lechuga, L. M. (2014) Trends and challenges of refractometric nanoplasmonic biosensors: A review. *Anal. Chim. Acta*, 806, 55-73.
4. Acimovic, S. S., Ortega, M. A., Sanz, V., Berthelot, J., Garcia-Cordero, J. L., Renger, J., Maerkl, S.J, Kreuzer, M.P., Quidant, R. (2014). LSPR chip for parallel, rapid, and sensitive detection of cancer markers in serum. *Nano Lett.*, *14*(5), 2636-2641.
5. Malic, L., Morton, K., Clime, L., Veres, T. (2013). All-thermoplastic nanoplasmonic microfluidic device for transmission SPR biosensing. *Lab Chip*, 13(5), 798-810.
6. Coskun, A. F., Cetin, A. E., Galarreta, B. C., Alvarez, D. A., Altug, H., & Ozcan, A. (2014). Lensfree optofluidic plasmonic sensor for real-time and label-free monitoring of molecular binding events over a wide field-of-view. *Sci. Rep.*, 4, 6789.

7. Cappi, G., Spiga, F. M., Moncada, Y., Ferretti, A., Beyeler, M., Bianchessi, M., Decosterd, L., Buclin, T., Guiducci, C. (2015). Label-free detection of tobramycin in serum by transmission-localized surface plasmon resonance. *Anal. Chem. 87*(10), 5278-5285.
8. Kabashin, A. V., Evans, P., Pastkovsky, S., Hendren, W., Wurtz, G. A., Atkinson, R., Pollard, R., Podolskiy, V.A., Zayats, A. V. (2009) Plasmonic nanorod metamaterials for biosensing. *Nat. Mater.* 8(11), 867-871.
9. Sreekanth, K. V., Alapan, Y., ElKabbash, M., Wen, A. M., Ilker, E., Hinczewski, M., Gurkan, U. A., Steinmetz, N.F., Strangi, G. (2016) Enhancing the Angular Sensitivity of Plasmonic Sensors Using Hyperbolic Metamaterials. *Adv. Opt. Mater.*, 4(11), 1767-1772.
10. Gartia, M. R., Hsiao, A., Pokhriyal, A., Seo, S., Kulsharova, G., Cunningham, B. T., Bond, T.Z., Liu, G. L. (2013) Colorimetric plasmon resonance imaging using nano lycurgus cup arrays. *Adv. Opt. Mater.* 1(1), 68-76.
11. Shen, Y., Zhou, J., Liu, T., Tao, Y., Jiang, R., Liu, M., Xiao, G., Zhu, J., Zhou, Z., Wang, X., Jin, C., Wang, J. (2013) Plasmonic gold mushroom arrays with refractive index sensing figures of merit approaching the theoretical limit. *Nat. Commun.* 4, 2381. doi:10.1038/ncomms3381.
12. Lee, K. L., Chen, P. W., Wu, S. H., Huang, J. B., Yang, S. Y., Wei, P. K. (2012) Enhancing surface plasmon detection using template-stripped gold nanoslit arrays on plastic films. *ACS Nano*,*6*(4), 2931-2939.
13. Chen, Y. (2015). Nanofabrication by electron beam lithography and its applications: A review. *Microelec. Eng.*, *135*, 57-72.
14. Kooy, N., Mohamed, K., Pin, L. T., Guan, O. S. (2014). A review of roll-to-roll nanoimprint lithography. *Nanoscale Res. Lett.*, *9*(1), 320.
15. Seo, J. H., Park, J. H., Kim, S. I., Park, B. J., Ma, Z., Choi, J., & Ju, B. K. (2014). Nanopatterning by laser interference lithography: applications to optical devices. *J. Nanosci. Nanotechnol*. *14*(2), 1521-1532.

16. Dou, X., Phillips, B. M., Chung, P. Y., Jiang, P. (2012) High surface plasmon resonance sensitivity enabled by optical disks. *Opt. Lett. 37*(17), 3681-3683.
17. Kaplan, B., Guner, H., Senlik, O., Gurel, K., Bayindir, M., Dana, A. (2009) Tuning optical discs for plasmonic applications. Plasmonics, 4(3), 237-243.
18. Lee, K. L., Huang, J. B., Chang, J. W., Wu, S. H., Wei, P. K. (2015). Ultrasensitive biosensors using enhanced Fano resonances in capped gold nanoslit arrays. *Sci. Rep.* 5, 8547, doi:10.1038/srep08547
19. Luk'yanchuk, B., Zheludev, N. I., Maier, S. A., Halas, N. J., Nordlander, P., Giessen, H., Chong, C. T. (2010). The Fano resonance in plasmonic nanostructures and metamaterials. *Nat. Mater.* 9(9), 707-715.
20. Offermans, P., Schaafsma, M. C., Rodriguez, S. R., Zhang, Y., Crego-Calama, M., Brongersma, S. H., Gómez Rivas, J. (2011) Universal scaling of the figure of merit of plasmonic sensors. *ACS Nano*, 5(6), 5151-5157.
21. Sultanova, N., Kasarova, S., Nikolov, I. (2009) Dispersion Proper ties of Optical Polymers. *Acta Phys. Pol. A* 116(4), 585-587.
22. Johnson, P. B., & Christy, R. W. (1972). Optical constants of the noble metals. *Phys. Rev. B*, 6(12), 4370-4379.
23. Soler, M., Estevez, M.-C., Villar-Vazquez, R., Casal, J.I., Lechuga, L.M. (2016) Label-free nanoplasmonic sensing of tumor-associate autoantibodies for early diagnosis of colorectal cancer. *Anal. Chim. Acta*, 93, 31-38.
24. Lee, K. L., Chang, C. C., You, M. L., Pan, M. Y., Wei, P. K. (2016) Enhancing the Surface Sensitivity of Metallic Nanostructures Using Oblique-Angle-Induced Fano Resonances, *Sci. Rep.* 6, 33126, doi:10.1038/srep33126.
25. Xiao, B., Pradhan, S. K., Santiago, K. C., Rutherford, G. N., Pradhan, A. K. (2015) Enhanced optical transmission and Fano resonance through a nanostructured metal thin film. *Sci. Rep.,* 5, 10393, doi:10.1038/srep10393.
26. Zhou, W., Odom, T. W. (2011) Tunable subradiant lattice plasmons by out-of-plane dipolar interactions. *Nat. Nanotechnol. 6*(7), 423-427.

27. Li, J., Chen, C., Lagae, L., Van Dorpe, P. (2015) Nanoplasmonic Sensors with Various Photonic Coupling Effects for Detecting Different Targets. *J. Phys. Chem. C*, *119*(52), 29116-29122.
28. Mazzotta, F., Johnson, T. W., Dahlin, A. B., Shaver, J., Oh, S. H., Höök, F. (2015) Influence of the evanescent field decay length on the sensitivity of plasmonic nanodisks and nanoholes. *ACS Photonics*, 2(2), 256-262.

Figure Legends

Figure 1. Chip integration and experimental set-up. (a) Photography of the integrated chip with the microfluidics channel and a Scanning Electron Microscopy (SEM) image (insert) of the Blu-ray based plasmonic nanostructures. (b) Experimental set-up including the optical detection scheme and the microfluidic system.

Figure 2. Optical Characterization of the plasmonic chips. Variation of the reflectance spectra in air (Ƞ=1.00) and water (Ƞ=1.33) of nanostructured plasmonic chip with 50 nm **(a)** and 100 nm **(b)** gold layer thickness varying the oblique light incidence angle.(c) Variation of the bulk sensitivity (black) and FWHM linewidth (red) as function of the angle of the incidence light for the two gold thickness..

Figure 3. FDTD Simulations of the proposed sensor. (a) Evaluated and simulated optical reflectance spectra under TM-polarization with a light incident angle of 70º for the two nanostructured plasmonic sensors fabricated. Simulated electric field distribution for the 50 nm (b) and 100 nm (c) gold thickness layer under TM-polarization for a light incidence angle of 70º.

Figure 4. Sensing performance evaluation. (a) Real-time sensograms of different solutions of glycerol for the two gold thickness layer chips fabricated. The insert shows the noise level of the sensor response. (b) Calibration curves and bulk sensitivity determination for the two gold thickness layer chips fabricated at a incidence angle of 70º.

Figure 5. Reproducibility evaluation of the fabrication process. (a) Reflectance spectra of nine different chips with 100 nm gold thickness obtained in three different fabrication batches. Spectra obtained under TM-polarized light with a fixed incident angle of 70º in air (Ƞ=1.00). (b) Resonant wavelengths and FHWM bandwidths of the nine chips. Mean values of 635.32 ± 0.61 nm and 10.12 ± 0.94 were obtained, respectively.

Figure 6. (a) Real-time sensograms showing the covalent immobilization of the protein GTF2b: activation of carboxylic SAM layer with EDC/NHS, attachment of the protein and blocking of unreacted groups; (b) sensograms showing the detection of the specific antibody at different concentrations (from 25 to 1000 ng.mL^{-1}) and control experiment; (c) calibration curve for the detection of the anti-GTF2b; (d) Effect of the PLL-PEG blocking step in the detection: green and orange lines shows the detection of antibody (800 ng/mL) without and with PLL-PEG layer, respectively; black line shows the nonspecific binding of 10% diluted serum ; blue line shows the detection of antibody (800 ng/mL) in 10% diluted serum.

Figure 1

Click here to download high resolution image

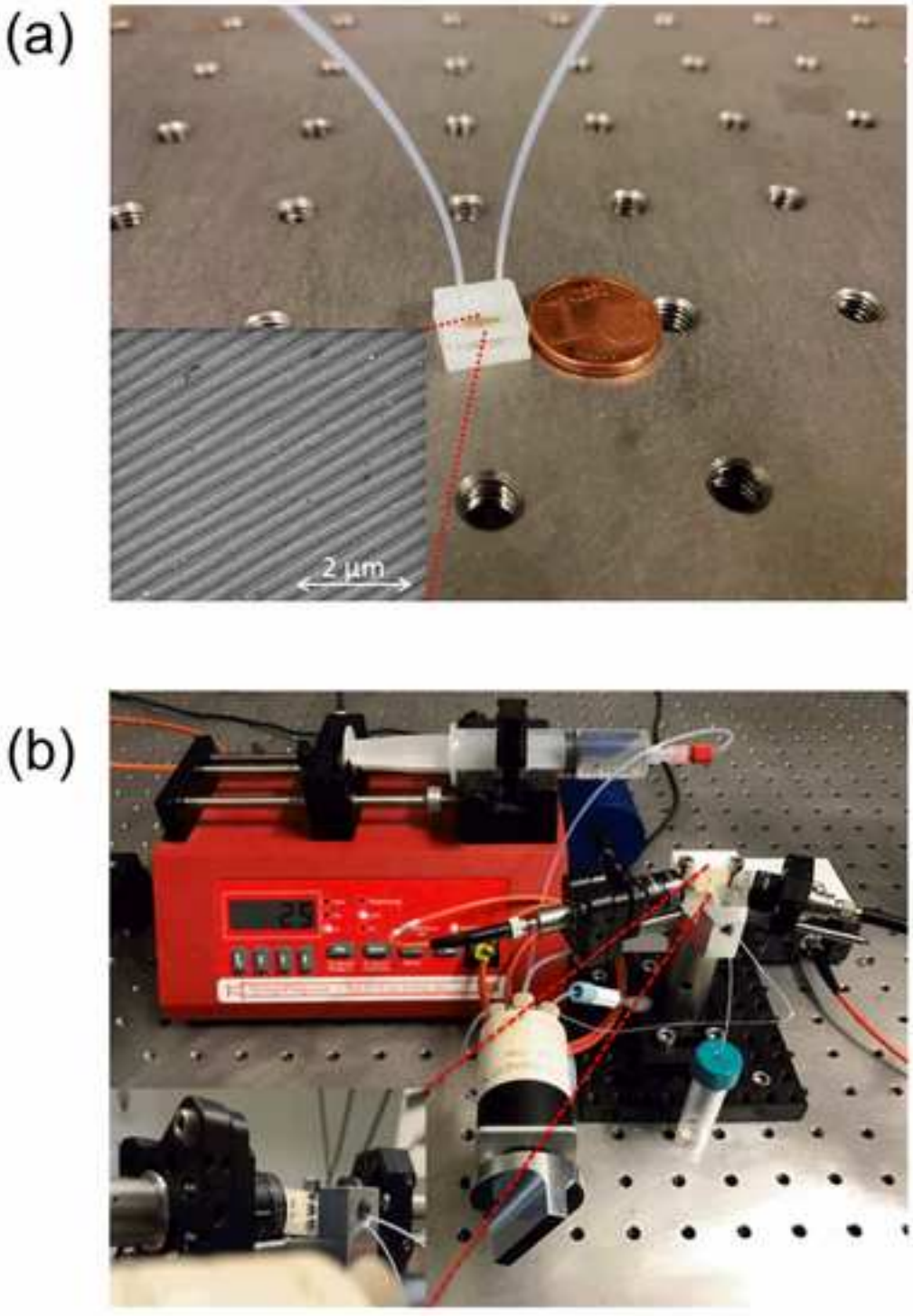

Figure 2

Click here to download high resolution image

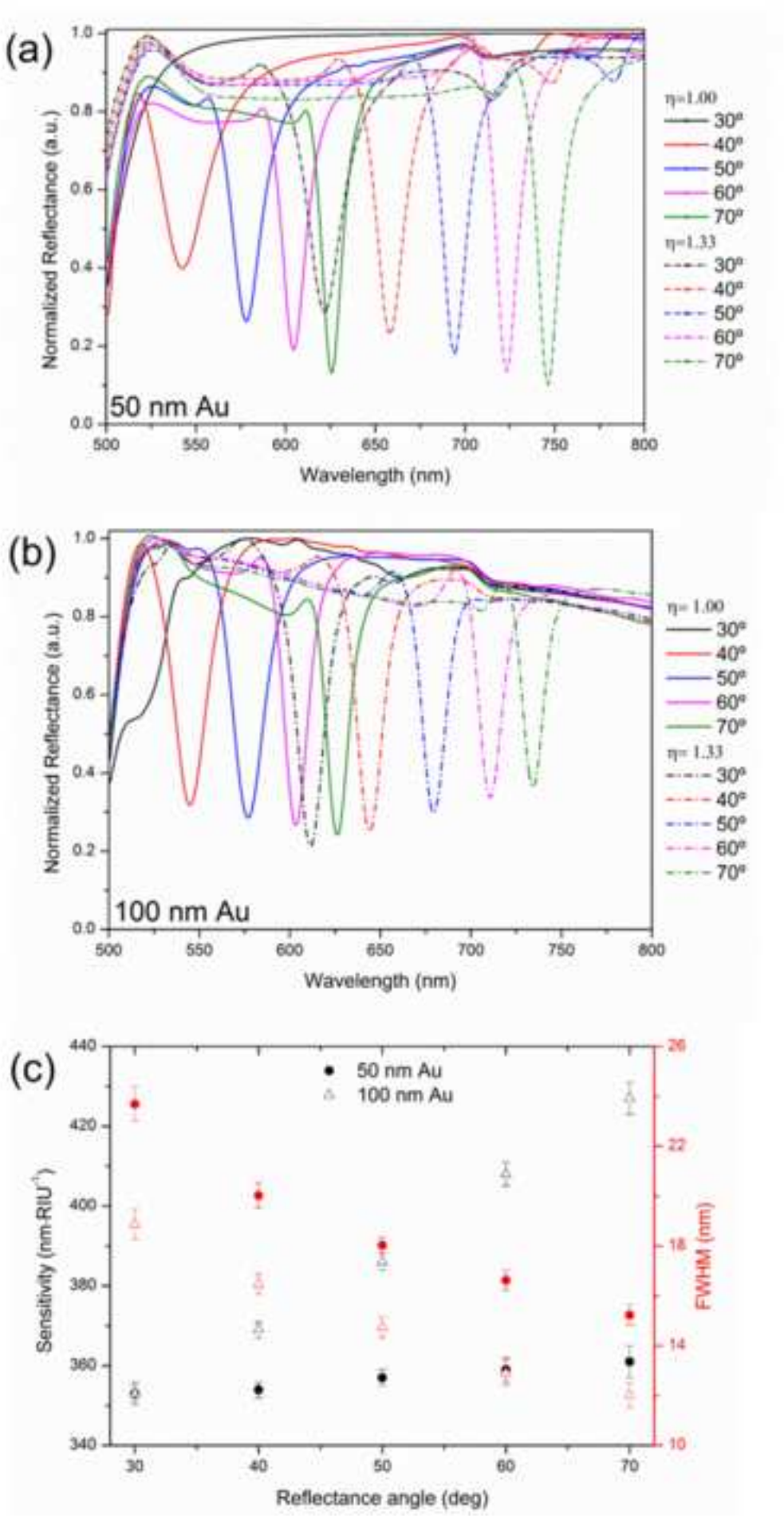

Figure 3

Click here to download high resolution image

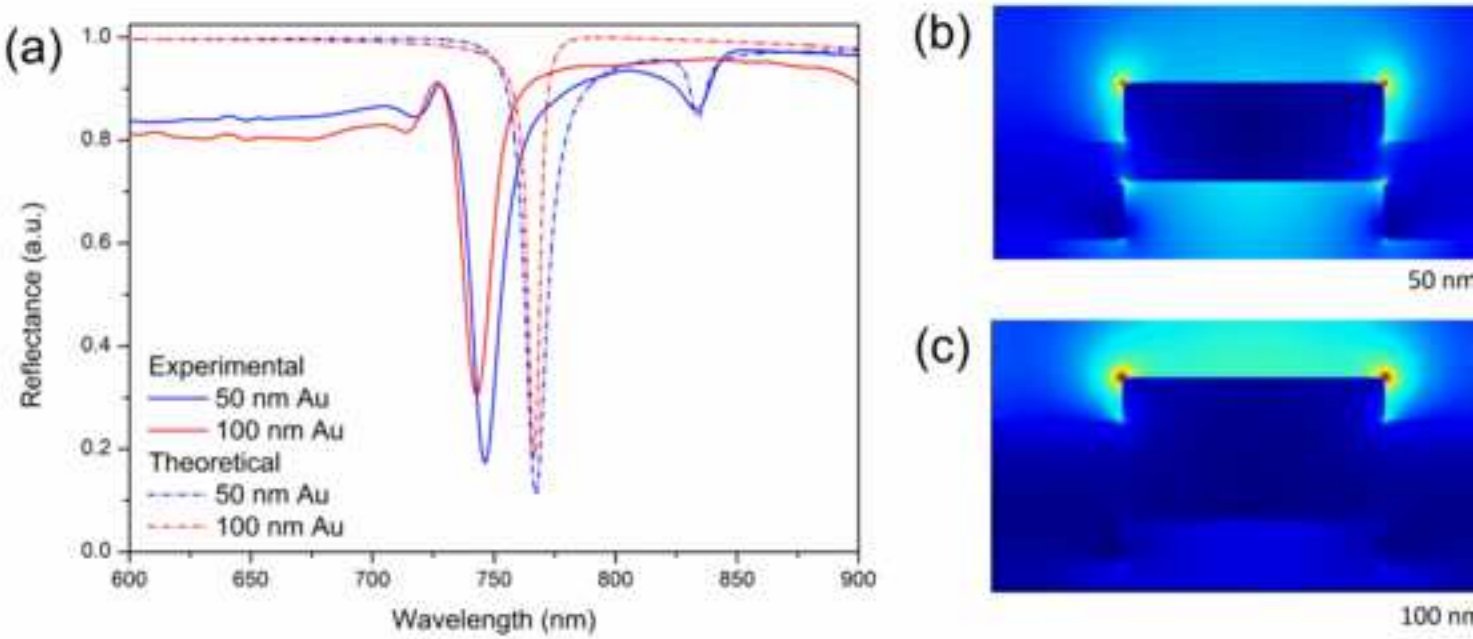

Figure 4

Click here to download high resolution image

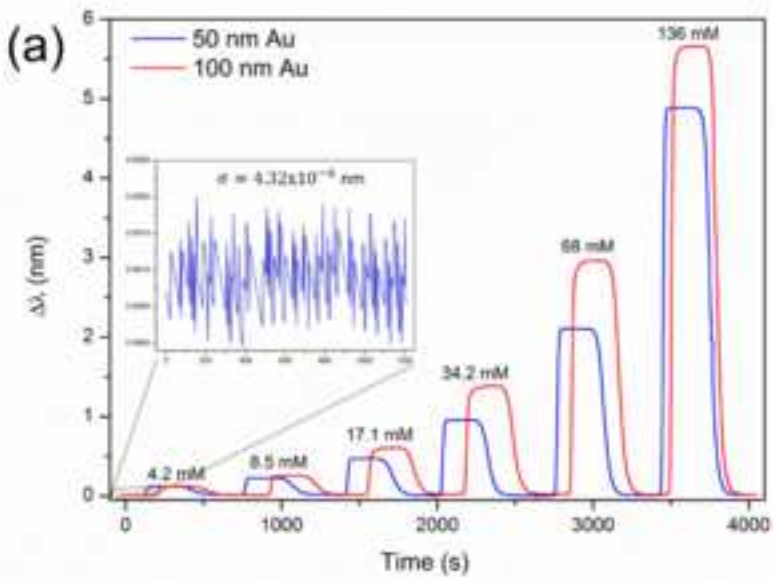

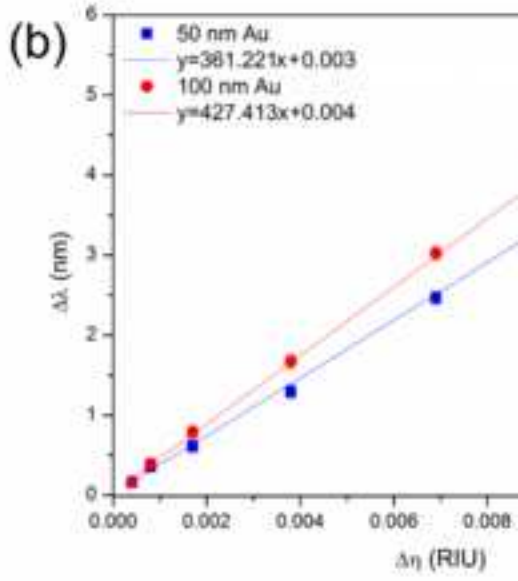

Figure 5

Click here to download high resolution image

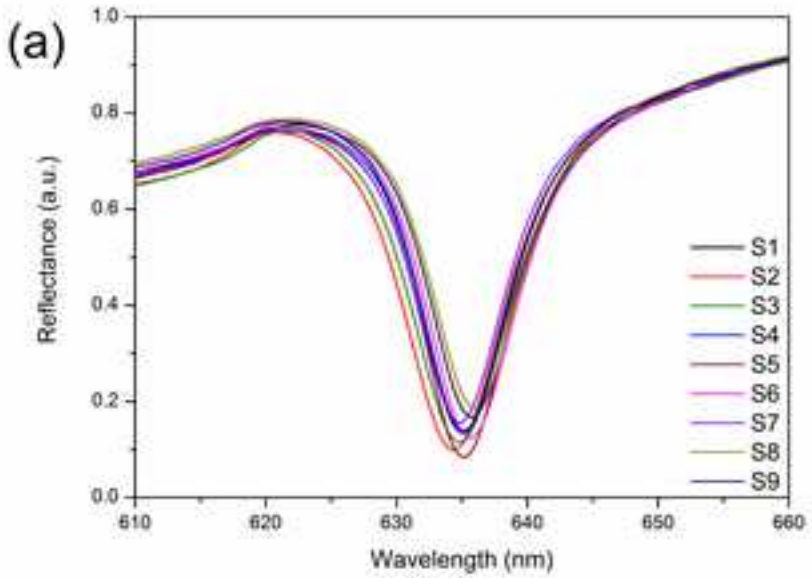

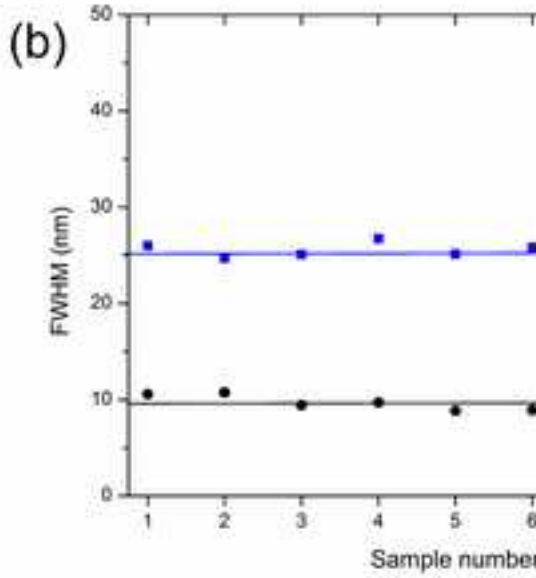

Figure 6

Click here to download high resolution image